Co- and Counterrotation of Magnetic Axes and Axial Ligands in Low-Spin Ferriheme Systems

Nikolai V. Shokhirev* and F. Ann Walker*

Contribution from the Department of Chemistry, University of Arizona, Tucson, Arizona 85721

Received July 8, 1997. Revised Manuscript Received October 24, 1997

Abstract: The orientation of the principal axes of the **g** tensor with respect to the relationship of axial ligand planes to the porphyrin nitrogens has been studied in the framework of the one-electron crystal field model for tetragonal and rhombic low-spin d^5 complexes such as ferriheme centers. All five d atomic orbitals were taken into account for two different ground-state electronic configurations, the "normal" $(d_{xy})^2(d_{xz},d_{yz})^3$ and the "novel" $(d_{xz},d_{yz})^4(d_{xy})^1$ configurations. The expressions for the **g** tensor, *g* values, and magnetic axes were derived on the basis of first-order perturbation theory. The conditions for co- and counterrotation of magnetic axes with rotation of planar axial ligands away from the porphyrin nitrogens toward the *meso* positions and beyond, as well as the order of *g* values, have been analyzed. It is found that counterrotation is the only possibility for the $(d_{xz},d_{yz})^4(d_{xy})^1$ configuration and that it is also by far more common for the $(d_{xy})^2(d_{xz},d_{yz})^3$ electron configuration. The possibilities of nonlinear co-/counterrotation are also explored. The predictions of this treatment are then compared to experimental results obtained from single-crystal EPR, glassy sample ESEEM, and solution NMR spectroscopic studies. It is clear that the majority of experimental systems reported thus far follow the major predictions of this treatment: Most systems exhibit angle-for-angle (linear) counterrotation of the **g** or χ tensor with rotation of planar axial ligands away for the N−Fe−N axes. Hence, knowing the structure of a model heme or heme protein, and in particular, the orientation of (fixed) axial ligand planes, one should be able to predict the approximate orientation of the in-plane magnetic axes. This knowledge provides a check on the values obtained in new solution NMR, single-crystal EPR or frozen solution ESEEM experiments.

Introduction

NMR spectroscopy has been used to determine the orientation of the **g** or χ tensor in a number of heme proteins, including cyanide-inhibited horseradish peroxidase,[1,2] several cyano-metmyoglobins,[3−7] ferricytochrome b_5,[4,8−12] and various cytochromes *c*.[13−15] These magnetic axis determinations have simply been reported in some cases, but recently Bertini and co-workers have shown that the orientation of the **g** or χ tensor and the dipolar (pseudocontact) shifts that result therefrom can be used as important additional constraints to help in the refinement of the 3D solution structure of the ferriheme protein.[16] It therefore becomes important to confirm that the magnetic axes determined from a series of NMR experiments are reasonable, for it appears to be easy to make errors in assigning magnetic axis directions, especially with respect to the heme moiety within the protein. One useful concept that has been mentioned recently by Turner[2,4,17] is that of counterrotation of the **g** or χ tensor with rotation of axial ligand planes (or methionine π-symmetry sulfur p orbital nodal plane) away from one or the other of the porphyrin N−Fe−N axes. In this concept, if the axial ligand plane is oriented at +20° from one of the N−Fe−N axes, the direction of the minimum *g* or χ value would be expected to be oriented at −20° to that same N−Fe−N axis, as illustrated diagrammatically in Figure 1. If this concept could be confirmed to be true in all cases, or if the possibilities and conditions for potential co- (+20°) and counter- (−20°) rotation could be deliniated, such predictions would provide an important check on experimentally determined **g** or χ tensors. The purpose of the present paper is to explore the concept, reasons and origins of counterrotation of the **g** or χ tensor and to delineate the conditions for co- and counterrotation.

Crystal field (CF) theory is widely used for the interpretation of electronic structure and magnetic properties of transition metal

(1) La Mar, G. N.; Chen, Z.; Vyas, K.; McPherson, A. D. *J. Am. Chem. Soc.* **1995**, *117*, 411.
(2) Pierattelli, R.; Banci, L.; Turner, D. L. *J. Biol. Inorg. Chem.* **1996**, *1*, 320.
(3) Emerson, S. D.; La Mar, G. N. *Biochemistry* **1990**, *29*, 1556.
(4) Banci, L.; Pierattelli, R.; Turner, D. L. *Eur. J. Biochem.* **1995**, *232*, 522.
(5) Yamamoto, Y.; Iwafune, K.; Nanai, N.; Osawa, A.; Chujo, R.; Suzuki, T. *Biochem. Jpn.* **1991**, *198*, 299.
(6) Qin, J.; La Mar, G. N.; Ascoli, F.; Brunori, M. *J. Mol. Biol.* **1993**, *231*, 1009.
(7) Banci, L.; Bertini, I.; Pierattelli, R.; Tien, M.; Vila, A. *J. Am. Chem. Soc.* **1995**, *117*, 8659.
(8) Keller, R. M.; Wüthrich, K. *Biochim. Biophys. Acta* **1972**, *285*, 326.
(9) (a) Williams, G.; Clayden, N. J.; Moore, G. R.; Williams, R. J. P. *J. Mol. Biol.* **1985**, *183*, 447. (b) Veitch, N. G.; Whitford, D.; Williams, R. J. P. *FEBS Lett.* **1990**, *269*, 297.
(10) McLachlan, S. J.; La Mar, G. N.; Lee, K.-B. *Biochim. Biophys. Acta* **1988**, *957*, 430.
(11) Guiles, R. D.; Basus, V. J.; Sarma, S.; Malpure, S.; Fox, K. M.; Kuntz, I. D.; Waskell, L. *Biochemistry* **1993**, *32*, 8329.
(12) Lee, K.-B.; McLachlan, S. J.; La Mar, G. N. *Biochim. Biophys. Acta* **1994**, *1208*, 22.
(13) Qi, P. X.; Beckman, R. A.; Wand, A. J. *Biochemistry* **1996**, *35*, 12275.
(14) Sukits, S. F.; Erman, J. E.; Satterlee, J. D. *Biochemistry* **1997**, *36*, 5251.
(15) Zhao, D.; Hutton, H. M.; Cusanovich, M. A.; MacKenzie, N. E. *Protein Sci.* **1996**, *5*, 1816.
(16) Banci, L.; Bertini, I.; Bren, K. L.; Cremonini, M. A.; Gray, H. B.; Luchinat, C.; Turano, P. *J. Biol. Inorg. Chem.* **1996**, *1*, 117.
(17) Turner, D. L. *Eur. J. Biochem.* **1995**, *227*, 829.

S0002-7863(97)02265-8 CCC: $15.00
Published on Web 01/22/1998

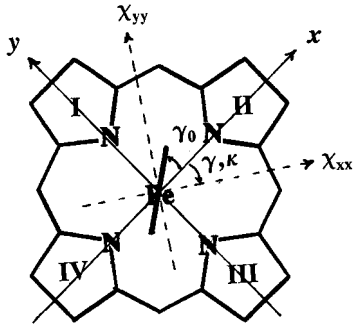

Figure 1. Heme ring with definition of axes (right-hand coordinate system) and axial ligand rotation angle, γ_0, used in this paper, and position of the magnetic axis χ_{xx} if counterrotation by an angle γ takes place. The angle κ is the sum of the Euler angles α and γ that define the relationship of the orientation of the magnetic susceptibility tensor to the molecular coordinate frame, assuming the Euler angle β is small, determined by NMR spectroscopic techniques. If the axial ligand plane is aligned along the *x* axis of the heme group, as shown, then the expectation is that the minimum magnetic susceptibility tensor component, χ_{xx}, will be aligned coincident with the axial ligand plane, along the molecular *x* axis. As the ligand rotates counterclockwise, χ_{xx} rotates in a clockwise direction in the majority of cases, or counterclockwise if corotation occurs.

complexes.[18−32] In particular, CF theory is used for the analysis of the electronic **g** tensors of paramagnetic transition metal complexes.[20,23−32] Typically, first-order perturbation theory has been used in this analysis, usually in the one-electron (or one-hole) formalism. With respect to low-spin d^5 systems, a treatment that considered only the three-level t_{2g} system (d_{xy}^2,d_{xz}^2,d_{yz}^1) was first developed by Griffith[19] and later elaborated into a more useful form by Taylor.[28] This one-electron crystal field treatment has been used for many years for the analysis of the EPR spectra of low-spin ferriheme complexes and proteins.[33]

Of the many investigations of the EPR spectra of low-spin d^5 complexes, particularly of ferriheme models and proteins, relatively few studies of the orientation of the **g** tensor with respect to the molecular frame have been reported. Among the existing reports are single-crystal EPR studies of two heme proteins[34−36] and a group of model ferrihemes,[30−32] and a number of NMR determinations,[1−17] as mentioned above. Recently we have investigated the magnetic field dependence of the intensity of the proton sum frequency peak in the ESEEM spectra of several model hemes to determine the orientation of the **g** tensor in glassy media.[37−39] In all but one[39] of these studies, g_{zz}, the component of the **g** tensor aligned most closely with the *z* molecular axis of the heme center, has been found to be the largest *g* value, indicating that the electron configuration of the low-spin d^5 center is $(d_{xy})^2(d_{xz},d_{yz})^3$. (The cases in which g_{zz} was found to be the smallest *g* value[39] are those which have been shown to have the novel $(d_{xz},d_{yz})^4(d_{xy})^1$ ground state.[40,41])

For the more common $(d_{xy})^2(d_{xz},d_{yz})^3$ systems, where g_{zz} is the largest *g* value, the orientation of g_{xx} was found to be close to the nodal plane of the imidazole ligand[1] or close to alignment along the methyl group of the coordinated methionine[34] in some proteins, while in others it has been found instead that g_{yy} is aligned along that direction.[10] Counterrotation of the **g** tensor with respect to the *hyperfine* tensor was first mentioned by Oosterhuis and Lang[27] for a system in which there were no planar ligands, $Fe(CN)_6^{3-}$. Although this work has frequently been quoted as justification of the counterrotation of the in-plane **g** tensor with rotation of axial ligands,[2,4,17] the need for counterrotation in that study appears to have resulted at least in part from the original assignment of the *g* values by these authors ($g_{zz} > g_{xx} > g_{yy}$).[27] The phenomenon of counter-rotation of the **g** tensor with respect to planar axial ligand rotation was later observed by Strouse and co-workers,[30−32] who showed that for ferriheme complexes in which axial ligands are aligned in parallel planes close to the N_2-Fe-N_4 axis of the porphyrin of Figure 1, g_{xx} is aligned along the nodal plane of the axial ligands, while if these ligands in parallel planes are rotated by 45° from the N_2-Fe-N_4 axis, g_{yy} is aligned along the nodal plane of these ligands, Figure 1. However, the concept of counterrotation of the **g** tensor has not been widely accepted or understood by most workers in the field, although, as mentioned above, it has recently been assumed to occur and used for the calculation of pseudocontact shifts of heme proteins.[2,4,17] As we will show, this assumption is, in fact, a good one, at least in the vast majority of cases.

In the studies in which counterrotation of the **g** tensor has been shown to occur by single-crystal EPR spectroscopic studies of model hemes,[30,31] only two angles, 0° and 45°, and only one electron configuration, $(d_{xy})^2(d_{xz},d_{yz})^3$, were observed. Extension of the one-electron treatment of Taylor[28] by Strouse and co-workers[30,31] also yields only the possibility of pure linear counterrotation of the **g** tensor with rotation of the axial ligands, or as we will define it, $\gamma = -\gamma_0$. We have reinvestigated this phenomenon using first-order perturbation theory, but have included all five d-orbital energy levels and have considered

(18) Ballhausen, C. J. *Introduction to Ligand Field Theory*; McGraw-Hill: New York, 1962.
(19) Griffith, J. S. *Proc. R. Soc. London, A* **1956**, *235*, 23.
(20) Griffith, J. S. *The Theory of Transition-Metal Ions*; Cambridge University Press: Cambridge, 1964.
(21) Dunn, T. M.; McClure, D. S.; Pearson, R. G. *Some Aspects of Crystal Field Theory*; Harper and Row: New York, 1965.
(22) Figgis, B. N. *Introduction of Ligand Fields*; Interscience: New York, 1966.
(23) McGarvey, B. R. Electron Spin Resonance of Transition-Metal Complexes; In *Transition Metal Chemistry*; Carlin, R. L., Ed.; M. Dekker: New York, 1966; Vol. 3, pp 89−201.
(24) Carrington, A.; McLachlan, A. D. *Introduction to Magnetic Resonance*; Harper and Row: New York, 1967.
(25) Abragam, A.; Bleaney, B. *Electron Paramagnetic Resonance of Transition Ions*; Clarendon Press: Oxford, 1970.
(26) Pilbrow, J. R. *Transition Ion Electron Paramagnetic Resonance*; Clarendon Press: Oxford, 1990.
(27) Oosterhuis, W. T.; Lang, G. *Phys. Rev.* **1969**, *178*, 439.
(28) Taylor, C. P. S. *Biochim. Biophys. Acta* **1977**, *491*, 137.
(29) Byrn, M. P.; Katz, B. A.; Keder, N. L.; Levan, K. R.; Magurany, C. J.; Miller, K. M.; Pritt, J. W.; Strouse, C. E. *J. Am. Chem. Soc.* **1983**, *105*, 4916.
(30) Quinn, R.; Valentine, J. S.; Byrn, M. P.; Strouse, C. E. *J. Am. Chem. Soc.* **1987**, *109*, 3301.
(31) Soltis, S. M.; Strouse, C. E. *J. Am. Chem. Soc.* **1988**, *110*, 2824.
(32) Inniss, D.; Soltis, S. M.; Strouse, C. E. *J. Am. Chem. Soc.* **1988**, *110*, 5644.
(33) (a) Blumberg, W. E.; Peisach, J. In *Structure and Bonding of Macromolecules and Membranes*; Chance, B., Yonetani, T., Eds.; Academic: New York, 1971; p 215. (b) Peisach, J.; Blumberg, W. E.; Adler, A. D. *Ann. N. Y. Acad. Sci.* **1973**, *206*, 310.
(34) Mailer, C.; Taylor, C. P. S. *Can. J. Biochem.* **1972**, *50*, 1048.
(35) Hori, H. *Biochim. Biophys. Acta* **1971**, *251*, 227.
(36) Peisach, J.; Blumberg, W. E.; Wyluda, B. J. *Eur. Biophys. Congr., Proc. 1st 1* **1971**, 109.
(37) Raitsimring, A. M.; Borbat, P.; Shokhireva T. Kh.; Walker, F. A. *J. Phys. Chem.* **1996**, *100*, 5235.
(38) Raitsimring, A. M.; Walker, F. A. *J. Am. Chem. Soc.* **1998**, *120*, 991 (accompanying paper).
(39) Raitsimring, A. M.; Polam, J. R.; Walker, F. A. Manuscript in preparation.
(40) Safo, M. K.; Walker, F. A.; Raitsimring, A. M.; Walters, W. P.; Dolata, D. P.; Debrunner, P. G.; Scheidt, W. R. *J. Am. Chem. Soc.* **1994**, *116*, 7760.
(41) Walker, F. A.; Nasri, H.; Turowska-Tyrk, I.; Mohanrao, K.; Watson, C. T.; Shokhirev, N. V.; Debrunner, P. G.; Scheidt, W. R. *J. Am. Chem. Soc.* **1996**, *118*, 12109.

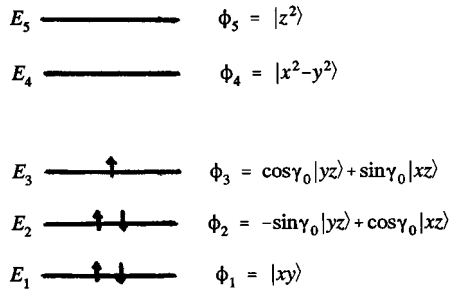

Figure 2. General energy level diagram of the d orbitals in a system of approximate D_{2h} symmetry, as defined by the coordination of one planar axial ligand or two planar axial ligands having some resultant orientation (i.e., the ligands are not oriented at perfect 90° angles).

arbitrary angles, γ_0, of orientation of the axial ligand (or the resultant orientation angle of two planar axial ligands that have relative orientations of less than 90°). In this case we find several interesting new features, including the possibility of and conditions for corotation of axial ligands and the **g** tensor, the nonlinear co- or counterrotation of axial ligands and **g** tensor, and the behavior of the **g** tensor for the "novel" $(d_{xz},d_{yz})^4(d_{xy})^1$ electronic ground state. These findings help to explain the seemingly strange observed orientations of the **g** tensors of heme proteins determined by EPR[34−36] or NMR[1−17] spectroscopy. More importantly, they confirm that counterrotation of the **g** tensor with rotation of axial ligands can be used in a predictive manner, as suggested previously by Turner.[2,4,17] In this work we intend to show that counterrotation is by far the most common behavior for both electron configurations, to delineate the conditions required for the less commonly observed corotation, and to stress the fact that the more common counterrotation situation can be used in a predictive manner.

The Model

The model complex consists of the central ion with five d orbitals in a crystal field of C_{4v} symmetry. The coordinate axes x and y are along the porphyrin nitrogen atoms (Figure 1), and the z axis is perpendicular to the porphyrin ring plane. This potential can be caused, e.g., by charges placed along $\pm x$, $\pm y$, and $\pm z$ axes). The effect of axial ligand(s) is modeled by a potential of the shape

$$U_{CF}(\phi) \propto z^2 \sin 2(\phi - \gamma_0) \tag{1}$$

Here γ_0 is the angle between the x axis and the plane of the axial ligand. The above potential can be modeled, e.g., by placing charges along the direction perpendicular to the axial ligand plane above and/or below the equatorial ligand plane. This is also the direction of the linear combination of d_{xz} and d_{yz} having higher energy. The electronic structure of the complex is schematically shown in Figure 2. When $\gamma_0 = 0$ (the axial ligand plane is along the x axis, Figure 1) the t_{2g}-type orbital with the highest energy is the pure d_{yz} orbital.

This order of levels in Figure 2 corresponds to the case of strong axial ligand crystal field. For some types and strengths of crystal field the orders of levels 4 and 5 and/or 1 and 2 can be inverted. However all these cases correspond to the electron configuration $\phi_1^2\phi_2^2\phi_3^1$.

For relatively weak axial ligand crystal field, or in cases of strongly π-accepting axial ligands, the d_{xy}-level can be above the d_{xz},d_{yz} levels.[40,41] This case corresponds to the configuration $\phi_2^2\phi_3^2\phi_1^1$.

Taking into account the spin−orbit (SO) interaction, we have the following one-electron Hamiltonian:

$$\hat{H} = \hat{H}^0 + \hat{V} = \hat{H}^0 + \lambda(\vec{s}\cdot\vec{l}) \tag{2}$$

The SO interaction V mixes the initial (zero-order) functions

$$\psi^0_{n\alpha} = \phi_n\alpha,\ \psi^0_{n\beta} = \phi_n\beta \tag{3}$$

The g Tensor. First-order perturbation theory gives the following expression for the components of the **g** tensor for the unpaired electron on the m-th level:[24,26]

$$g^1_{\mu\nu} = g_e\delta_{\mu\nu} - \sum_{m\neq n}\frac{\langle\phi_m|1_\mu|\phi_n\rangle\langle\phi_m|1_\nu|\phi_n\rangle}{E^0_n - E^0_m},\ \mu, \nu = x, y, z \tag{4}$$

Here g_e is the free electron g value.

Configuration $\phi_1^2\phi_2^2\phi_3^1$. Applying the above equation to $m = 3$ of the model complex, we obtain

$$g_{xx} = g_e + 2\lambda\left(\frac{s^2}{\Delta_{31}} - \frac{c^2}{\Delta_{43}} - 3\frac{c^2}{\Delta_{53}}\right)$$

$$g_{yy} = g_e + 2\lambda\left(\frac{c^2}{\Delta_{31}} - \frac{s^2}{\Delta_{43}} - 3\frac{s^2}{\Delta_{53}}\right)$$

$$g_{zz} = g_e + 2\frac{\lambda}{\Delta_{32}},\ g_{xz} = g_{yz} = 0$$

$$g_{xy} = -2\lambda\left(\frac{sc}{\Delta_{31}} + \frac{sc}{\Delta_{43}} - 3\frac{sc}{\Delta_{53}}\right) \tag{5}$$

Configuration $\phi_2^2\phi_3^2\phi_1^1$. Equation 4 for $m = 1$ gives

$$g_{xx} = g_e + 2\lambda\left(\frac{c^2}{\Delta_{12}} + \frac{s^2}{\Delta_{13}}\right)$$

$$g_{yy} = g_e + 2\lambda\left(\frac{s^2}{\Delta_{12}} + \frac{c^2}{\Delta_{13}}\right)$$

$$g_{zz} = g_e - \frac{2\lambda}{\Delta_{41}},\ g_{xz} = g_{yz} = 0$$

$$g_{xy} = 2\lambda\left(\frac{sc}{\Delta_{12}} - \frac{sc}{\Delta_{13}}\right) \tag{6}$$

In the above expressions (eqs 5 and 6) and those below

$$\Delta_{nm} = E_n - E_m,\ c = \cos\gamma_0,\ s = \sin\gamma_0 \tag{7}$$

Principal Axis Orientation. The principal axes of the **g** tensor, by definition, can be obtained from the eigenvalue problem:

$$\hat{g}\cdot\vec{c}_n = g_n\vec{c}_n,\ n = 1, 2, 3 \tag{8}$$

Configuration $\phi_1^2\phi_2^2\phi_3^1$. For our model, $\vec{c}_3$ coincides with the z axis, $\vec{c}_1$ and $\vec{c}_2$ are in the xy plane and are turned by the angle γ relative to the x and y axes correspondingly:

$$\tan 2\gamma = \frac{2g_{xy}}{g_{yy} - g_{xx}} = \frac{\xi}{\eta}\tan 2\gamma_0 \tag{9}$$

where

$$\xi = \frac{3}{\Delta_{53}} - \frac{1}{\Delta_{43}} - \frac{1}{\Delta_{31}}, \eta = \frac{3}{\Delta_{53}} + \frac{1}{\Delta_{43}} + \frac{1}{\Delta_{31}} \quad (10)$$

The corresponding g values are

$$g_{1,2} = g_e + \lambda\left(\frac{1}{\Delta_{31}} - \frac{1}{\Delta_{43}} - \frac{3}{\Delta_{53}} \mp \sqrt{\eta^2 \sin^2 2\gamma_0 + \xi^2 \cos^2 2\gamma_0}\right)$$

$$g_3 = g_e + \frac{2\lambda}{\Delta_{32}} \quad (11)$$

Note that at the same level of approximation:

$$\sum_{n=1}^{3} g_n^2 = 3g_e^2 + 4g_e\lambda\left(\frac{1}{\Delta_{32}} + \frac{1}{\Delta_{31}} - \frac{1}{\Delta_{43}} - \frac{3}{\Delta_{53}}\right) \quad (12)$$

Configuration $\phi_2^2\phi_3^2\phi_1^1$. Again $\vec{c}_3$ coincides with the z axis, $\vec{c}_1$ and $\vec{c}_2$ are in the xy plane and are turned by the angle $\gamma = -\gamma_0$ relative to the x and y axes. The corresponding g values are

$$g_1 = g_e + \frac{2\lambda}{\Delta_{12}}, g_2 = g_e + \frac{2\lambda}{\Delta 13}, g_3 = g_e - \frac{8\lambda}{\Delta_{41}} \quad (13)$$

and

$$\sum_{n=1}^{3} g_n^2 = 3g_e^2 + 4g_e\lambda\left(\frac{1}{\Delta_{13}} + \frac{1}{\Delta_{12}} - \frac{4}{\Delta_{41}}\right) \quad (14)$$

In all cases in-plane g values are labeled so that $g_1 < g_2$.

g Tensor Analysis. Configuration $\phi_1^2\phi_2^2\phi_3^1$. According to equations 9−11, the rotation of the axial ligand causes both the rotation of the axes $\vec{c}_1$ and $\vec{c}_2$ and changes the values of g_1 and g_2. In general, $|\xi/\eta| < 1$. This means that near the x and y axes (the normal to the axial plane directed to the porphyrin nitrogen atoms) the rotation of the in-plane **g** tensor axes is less than the rotation of the axial ligand: $|\delta\gamma| < |\delta\gamma_0|$ (see eq 9 and curves 1 and 2 in Figure 3). Near the *meso* directions ($\gamma_0 = \pm 45°$) the rate of change in the orientation of magnetic axes is larger than the change in orientation of the axial ligand: $|\delta\gamma| < |\delta\gamma_0|$ (Figure 3, curves 1 and 2). This nonlinear behavior is observed when all five, rather than only the three lowest, d orbitals, are within reasonable energy of each other (perhaps $16-25\lambda$ or so, where λ is the spin−orbit coupling constant, or $E_5 - E_1 \geq 10\,000$ cm^{-1}, considerably smaller at the lower limit than expected for normal low-spin ferriheme systems, and hence probably not a physically reasonable case for low-spin ferrihemes, although possibly reasonable for other low-spin d^5 systems).

According to equations 9 and 10, the rotation of the axes $\vec{c}_1$ and $\vec{c}_2$ in the same direction as the axial ligand plane (corotation) will occur if $\xi > 0$ or

$$\frac{\Delta_{53}}{\Delta_{31}} < \frac{3}{1 + \frac{\Delta_{31}}{\Delta_{43}}} \quad (15)$$

The regions of co- and counterrotation are displayed in Figure 4. Condition 15 is satisfied below curve 1. Above the diagonal straight line 2, $E(d_{z^2}) > E(d_{x^2-y^2})$. This case is consistent with co-rotation and corresponds to the closed area between curves 1 and 2.

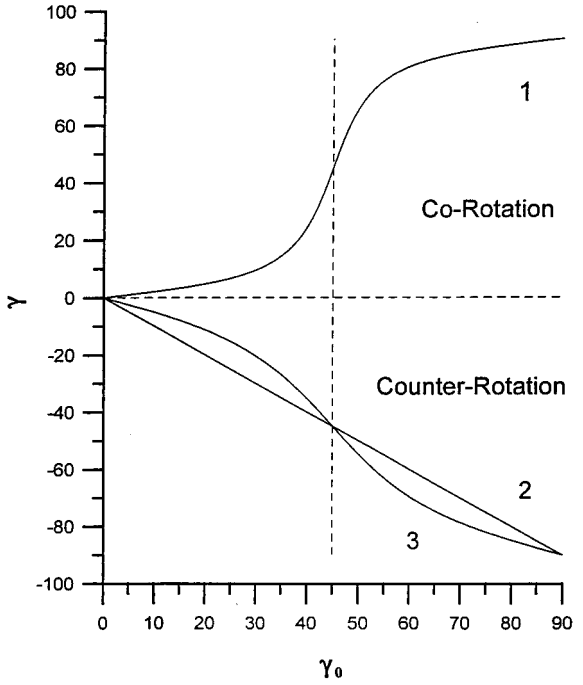

Figure 3. The dependence of the magnetic axes rotation angle γ on the axial ligand rotation angle γ_0 (see eq 9). Curve 1: $\xi/\eta = 0.2$; corotation of axial ligands with magnetic axis rotation delayed near $\gamma_0 = 0$ and 90°and accelerated near $\gamma_0 = 45°$. Curve 2: $\xi/\eta = -1$; pure angle-for-angle counterrotation. Curve 3: $\xi/\eta = -0.5$; counterrotation delayed near $\gamma_0 = 0$ and 90°and accelerated near $\gamma_0 = 45°$.

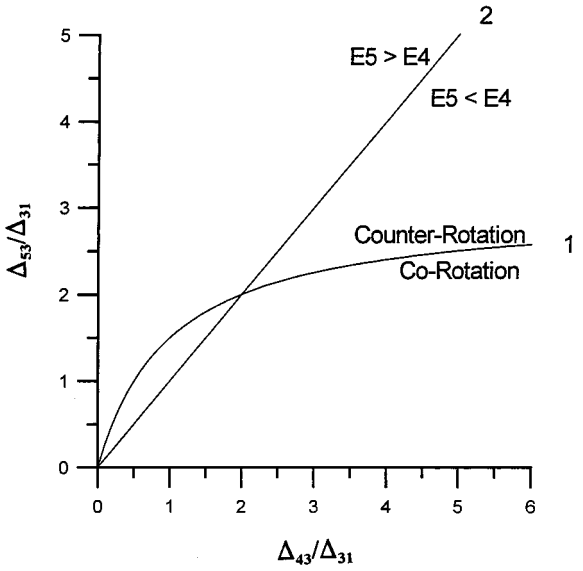

Figure 4. The regions of co- and counterrotation in a reduced energy splitting plane. The orbital energy parameters below and above curve 1 correspond to the cases of co- and counterrotation, respectively. Curve 2 divides the plane of parameters into the region of the "normal", $E_5 > E_4$ (above), and inverted, $E_4 > E_5$ (below), order of levels. The only allowed region for corotation is in the small area bounded by the crossing points of curves 1 and 2.

The most commonly observed orientations of axial ligands are close to $\gamma_0 = 0$ (or $\gamma_0 = \pm 90°$) and $\gamma_0 = \pm 45°$. Let us consider these cases in more detail.

The Case $\gamma_0 = 0$, $\gamma = 0$. The plane of the axial ligand eclipses two opposite equatorial ligands. The axis $\vec{c}_1$ is parallel

to the axial ligand plane, $\vec{c}_2$ is perpendicular to the plane. The $g_{1,2}$ values are

$$g_1 = g_e - 2\lambda\left(\frac{1}{\Delta_{43}} + \frac{3}{\Delta_{53}}\right)$$

$$g_2 = g_e + \frac{2\lambda}{\Delta_{31}} \tag{16}$$

If the d_{xy}-level is lowest in energy in the $t_{2\,g}$-subset ($E_1 < E_2 < E_3$) then the g-values are ordered in the following way:

$$g_3 > g_2 > g_e > g_1 \tag{17}$$

This is the most commonly observed order of g values, which is observed for most of the low-spin ferriheme centers that conform to the "C" (His-Met), "B" (His-His), "H" (deprotonated His-His), "O" (His-OH), and probably also "P" (Cys^--L) regions of the Blumberg−Peisach "Truth Diagrams".[33]

If $E_2 < E_1 < E_3$ then the order is

$$g_2 > g_3 > g_e > g_1 \tag{18}$$

This order has not, to our knowledge, been observed experimentally.

The Case $\gamma_0 = 45°$. The Plane of the Axial Ligand Is Along Two of the *Meso* Positions of the Porphyrin Ring. There can be two subcases: co- and counterrotation.

(1) Corotation: $\xi > 0$, $\gamma = 45°$. The axis $\vec{c}_1$ is parallel to the axial ligand plane, $\vec{c}_2$ is perpendicular to the plane. The $g_{1,2}$ values are

$$g_1 = g_e - 2\lambda\left(\frac{3}{\Delta_{53}} - \frac{1}{\Delta_{31}}\right)$$

$$g_2 = g_e - \frac{2\lambda}{\Delta_{43}} \tag{19}$$

The order of g values is the following

$$g_3 > g_e > g_2 > g_1 \tag{20}$$

This is the order observed for the "large g_{max}" centers of model hemes having imidazole or high-basicity pyridine ligands in nearly perpendicular planes,[42−44] as well as for the *b* hemes of the membrane-bound cytochrome *b* of mitochondrial complex III[45−47] and those of the similar centers of chloroplast cytochrome b_6.[48] In the model heme complexes having "perpendicular" orientations of axial ligands whose crystal structures have been reported, the actual relative orientations of the axial ligands always deviate by at least 1−4°,[32,43,44,49,50] and sometimes by more than that, from perfect 90° orientations, thus creating at least a small residual "parallel" component of combined ligand plane orientation. Because of the Jahn−Teller effect, that "encourages" a complex with a degenerate orbital state to distort to remove the degeneracy, it is likely that two planar axial ligands will never be found in perfect 90° orientations in low-spin ferriheme model complexes (or heme proteins).

(2) Counterrotation: $\xi < 0$, $\gamma_0 = 45°$, $\gamma = -45°$. The axis $\vec{c}_1$ is perpendicular to the axial ligand plane, and $\vec{c}_2$ is parallel to the plane. The $g_{1,2}$ values are

$$g_1 = g_e - \frac{2\lambda}{\Delta_{43}}$$

$$g_2 = g_e + 2\lambda\left(\frac{1}{\Delta_{31}} - \frac{3}{\Delta_{53}}\right) \tag{21}$$

The following orders of g values may occur:

(a) if $\Delta_{53} > 3\Delta_{31}$ (strong axial ligand CF) and

$$E_1 - \frac{3\Delta_{32}\Delta_{31}}{\Delta_{53}} < E_2 < E_3 \tag{22}$$

then

$$g_3 > g_2 > g_e > g_1 \tag{23}$$

For low-spin ferriheme "normal rhombic" systems such as the "B" centers of heme proteins, calculations based on the Taylor formalism[28] provide estimates of the separation of $\Delta_{31} \approx 4-5\lambda$, or 1000−2000 cm^{-1}, depending on the choice of the value of the spin−orbit coupling constant, λ. This would require $\Delta_{53} > 12-15\lambda$, or greater than 3000−6000 cm^{-1}, or $\Delta_{51} > 4000-8000$ cm^{-1}. These are easily achievable minimum energy separations for almost any CF; the actual energy separations Δ_{51} for low-spin ferriheme systems are generally larger than 20 000 cm^{-1}.[51]

(b) if the axial CF is still strong but

$$E_2 + \frac{3\Delta_{32}\Delta_{31}}{\Delta_{53}} < E_1 < E_3 \tag{24}$$

then

$$g_2 > g_3 > g_e > g_1 \tag{25}$$

Again, as mentioned above, to our knowledge this order has not been observed experimentally.

(c) In the case of weak axial CF, $\Delta_{53} < 3\Delta_{31}$ and

$$g_3 > g_e > g_2 > g_1 \tag{26}$$

This is again the order found for the single-feature "large g_{max}" centers of model hemes having imidazole or high-basicity pyridine ligands in nearly perpendicular planes[42−44] and the *b* hemes of the membrane-bound complex III[45−47] and chloroplasts.[48] "Large g_{max}" EPR spectra are also possible for cases a and b, for which the parameters of the more anisotropic types of cytochromes *c*[52] are also representative of this order of g values ($g_3 \approx 3.3-3.45$, $g_2 \approx 2.0-2.1$, $g_1 \approx 0.1-0.8$).

Configuration $\phi_2^2\phi_3^2\phi_1^1$. For this configuration and the first-order approximation, our model always predicts only pure counterrotation (line 2 in Figure 3). For any angle of rotation

(42) Walker, F. A.; Huynh, B. H.; Scheidt, W. R.; Osvath, S. R. *J. Am. Chem. Soc.* **1986**, *108*, 5288.
(43) Safo, M. K.; Gupta, G. P.; Walker, F. A.; Scheidt, W. R. *J. Am. Chem. Soc.* **1991**, *113*, 5497.
(44) Safo, M. K.; Gupta, G. P.; Watson, C. T.; Simonis, U.; Walker, F. A.; Scheidt, W. R. *J. Am. Chem. Soc.* **1992**, *114*, 7066.
(45) Erecinska, M.; Oshino, R.; Oshino, N.; Chance, B. *Arch. Biochem. Biophys.* **1973**, *157*, 431.
(46) Leigh, J. S.; Erecinska, M. *Biochim. Biophys. Acta* **1975**, *387*, 95.
(47) Salerno, J. C. *J. Biol. Chem.* **1984**, *259*, 2331.
(48) Salerno, J. C. *FEBS Lett.* **1983**, *162*, 257.
(49) Scheidt, W. R.; Kirner, J. L.; Hoard, J. L.; Reed, C. A. *J. Am. Chem. Soc.* **1987**, *109*, 1963.
(50) Munro, O. Q.; Marques, H. M.; Debrunner, P. G.; Mohanrao, K.; Scheidt, W. R. *J. Am. Chem. Soc.* **1995**, *117*, 935.
(51) Gouterman, M. In *The Porphyrins*; Dolphin, D., Ed.; Academic Press: New York, 1978; Vol. III, pp 1−165.
(52) Gadsby, P. M. A.; Hartshorn, R. T.; Moura, J. J. G.; Sinclair-Day, J. D.; Sykes, A. G.; Thomson, A. J. *Biochim. Biophys. Acta* **1983**, *722*, 137.

the g values are given by eq 14. The order of g values is always the following:

$$g_1 > g_2 > g_e > g_3 \tag{27}$$

However the assignment of axes depends on the orientation of the axial ligand plane relative to the equatorial ligands:

(1) In the case $\gamma_0 = 0$, $\gamma = 0$, the plane of the axial ligand eclipses two of the equatorial ligands. The axis $\vec{c}_1$ is parallel to the axial ligand plane, $\vec{c}_2$ is perpendicular to the plane.

(2) If $\gamma_0 = 45°$ the plane of the axial ligand is oriented along two opposite *meso* positions. The axis $\vec{c}_1$ is perpendicular to the axial ligand plane, $\vec{c}_2$ is parallel to the plane.

Typical systems that have this $\phi_2^2\phi_3^2\phi_1^1$ configuration include the model heme complexes, $[TPPFe(4\text{-}CNPy)_2]ClO_4$,[53] $[TPPFe(t\text{-}BuNC)_2]ClO_4$,[41] and $[OEPFe(t\text{-}BuNC)_2]ClO_4$,[41] and probably the majority of the low-spin Fe(III) centers of reduced hemes, including low-spin iron(III) chlorins, isobacteriochlorins and β-oxoporphyrins such as cytochromes *d*.[53] (However, the three model compounds mentioned have strictly axial symmetry, with the axial ligands either in nearly perfectly perpendicular planes (4-CNPy) or else no planes at all (*t*-BuNC), and are thus of less interest to the present study of the effect of *planar* ligands in parallel, or at least not strictly perpendicular, planes on the orientation of the in-plane magnetic axes.) Unfortunately, to date there have been no reports of determinations of the orientation of the **g** tensor of hydroporphyrin or β-oxoporphyrin ferriheme centers, where the hydroporphyrinate-type ligand imposes the nonaxial symmetry of the **g** tensor, by single-crystal EPR or other methods.

Discussion

We begin by pointing out that the Griffith−Taylor approach[19,28] is based solely on the effects of orbital mixing due to spin−orbit coupling and (i) is restricted to the case of three levels (the t_{2g} levels of octahedral symmetry) and (ii) does not take into account many-electron effects. We have extended the Griffith−Taylor treatment to include all five d orbitals and to include first-order perturbation theory corrections to the g values. However, we are still using a one-electron (one hole) approach. In a later paper that deals with many-electron effects[54] the equations for calculating the g values will be further refined, but the one-electron treatment is sufficiently accurate to show the trends and tendencies for orientation of the **g** tensor of interest to the present study. First-order perturbation theory makes the zeroth-order correction in the orientation of $\vec{c}_1$ and $\vec{c}_2$ because it lifts the degeneracy of the in-plane g values (eqs 9 and 10), but it can predict only the tendency in g values, but not their exact magnitude, and by definition, it allows one to describe only small deviations from the free-electron g values. We will now consider several applications of our treatment to experimental data obtained from single-crystal EPR, glassy solution ESEEM, and homogeneous solution NMR measurements.

Magnetic Axis Orientations of Model Hemes Determined by Single-Crystal EPR Techniques. The single-crystal X-ray and EPR data of Strouse's group[30−32] first showed experimentally the phenomenon of counter-rotation of the **g** tensor with axial ligand rotation away from a porphyrin N−Fe−N axis. For the study of the substituted imidazole, bis(cis-methylurocanate) (cMU), the two molecules of $[TPPFe(cMU)_2]^+SbF_6^-$ found in the unit cell both had inversion centers, indicating that in both molecules the axial ligands were in parallel planes.[30] For molecule B the imidazole planes were rotated by $\gamma_0 = 15°$ from the x axis (N_2−Fe−N_4 direction, Figure 1) while the smaller in-plane g value (g_{xx}) was rotated by $\gamma = -11.2°$ from that axis. For molecule A the imidazole planes were rotated by $\gamma_0 = 29°$ while the smaller in-plane g value was rotated by $\gamma = -27.7°$. This suggests an approximately equal but opposite rotation of the **g** tensor with axial ligand rotation, although the smaller angle of rotation of the **g** tensor of molecule B *could* suggest the lagging phenomenon shown in Figure 3 for small angles of γ_0. For $[TPPFe(ImH)_2]^+Cl^-\cdot CHCl_3\cdot H_2O$,[31,55] again, two molecules with inversion centers are found in the unit cell, one of which has $\gamma_0 = 5°$ and $\gamma = -3°$ while the other has $\gamma_0 = 41°$ and $\gamma = -42°$,[31] Figure 1. Hence, for these model complexes there is good agreement between the experimental data and our predictions (Figure 3), and on the whole, linear counterrotation appears to occur for these complexes. For the "large g_{max}" species [TPPFe(CN)(Py)]; however, the pyridine plane is oriented at an angle $\gamma_0 = 41°$,[56] while the larger and smaller in-plane g values are oriented along the N−Fe−N directions ($\gamma = 0°$).[32] The authors pointed out that it appeared that the pyridine ligand contributes almost nothing to the observed rhombic splitting.[32] The cylindrical strong-field cyanide ligand can impose no directionality on the in-plane **g** tensor (unless it binds in a bent fashion, which is not the case in this complex), and this "large g_{max}" species with near degeneracy of d_{xz} and d_{yz} apparently distorts from purely tetragonal symmetry in a "noncommittal" sort of way, by placing the two in-plane magnetic axes at approximately 45° angles to the pyridine plane. This is likely not the case for the histidine cyanide-ligated heme proteins, including metMbCN, HRPCN, LiPCN, and M80A cytochrome *c* CN discussed below, since imidazole is a stronger field ligand than pyridine.

Magnetic Axis Orientations of Model Hemes Determined by Pulsed EPR Techniques. ESEEM studies carried out in this laboratory,[37−39] which have allowed determination of the orientation of the **g** tensor of low-spin ferriheme species in glassy media by use of the angle selection inherent in ESEEM measurements as a function of magnetic field, have shown marked differences in the orientation of the major in-plane g value with respect to the plane of the (parallel) axial ligands. For $[TPPFe(PzH)_2]^+ClO_4^-$,[37] the smaller in-plane g value is aligned parallel to the plane of the axial pyrazole ligands, while for $[OEPFe(4\text{-}NMe_2Py)_2]^+ClO_4^-$ the smaller in-plane g value is aligned perpendicular to the plane of the axial 4-(dimethylamino)pyridine ligands;[38] for $[OEPFe(ImH)_2]^+Cl^-$ an intermediate situation was found, in which the two in-plane g values are aligned at ±45° to the perpendicular to the axial imidazole ligands.[38] The structures of all three complexes have been determined in the solid state, and for the two OEP complexes the axial ligands are in parallel planes, with the ligands of the bis-imidazole complex lying close to the pyrrole ring II,IV nitrogen axis ($\gamma_0 = 7°$),[57] and those of the bis-4-(dimethylamino)pyridine complex lying close to opposite *meso* positions of the OEP ring ($\gamma_0 = 41°$).[43] Thus, for these two cases we have $\gamma_0 = 7°$, $\gamma \sim 45°$ for the bis-imidazole complex and $\gamma_0 = 41°$, $\gamma \sim -45°$ for the bis-4-(dimethylamino)pyridine complex. The latter represents very good correspondence between the experimental data and our theoretical predictions, while the former

(53) Cheesman, M. R.; Walker, F. A. *J. Am. Chem. Soc.* **1996**, *118*, 7373.
(54) Shokhirev, N. V.; Walker, F. A. Manuscript in preparation.
(55) Scheidt, W. R.; Osvath, S. R.; Lee, Y. J. *J. Am. Chem. Soc.* **1987**, *109*, 1958.
(56) Scheidt, W. R.; Lee, Y. J.; Luangdilok; Haller, K. J.; Anzai, K.; Hatano, K. *Inorg. Chem.* **1983**, *22*, 1516.
(57) Takenaka, A.; Sasada, Y.; Watanabe, E.-I.; Ogoshi, H.; Yoshida, Z.-I. *Chem. Lett. Jpn.* **1972**, 1235.

does not. If counterrotation of the **g** tensor with rotation of axial ligands away from the porphyrin nitrogens occurs for the bis-imidazole complex, it is tempting to conclude that the imidazole ligands take up rather different orientations of about 22° from the N_2-Fe-N_4 axis in frozen solution rather than the 7° observed in the crystalline state[57] (Figure 1). This is not difficult to imagine, for we have shown elsewhere that the energy barrier to ligand rotation is very low,[58−60] especially for nonhindered imidazoles.[60]

For the bis-pyrazole complex, the crystal structure has not been published but is said to have the two pyrazole ligands *not* in parallel planes, but rather at dihedral angles of 45° and 54° for the two independent molecules, with the average ligand plane orientation of the two ligands lying very close to the porphyrin nitrogens of two opposite pyrrole rings for the two independent molecules in the unit cell.[61] The ESEEM data are sensitive to the extent of only about ±20° to ligand orientation,[37] so it is not possible to determine whether the ligands have their crystallographically observed orientations in frozen solution, or adopt parallel ligand orientations, but in either case, our experimental results are consistent with $\gamma = 0°$ and hence $\gamma_0 = 0°$, at least for the *average* ligand plane orientation.

Magnetic Axis Orientations of Ferriheme Models of Heme Proteins Determined by Solution NMR Spectroscopic Techniques. Looking back at our calculations of the rhombic dipolar shifts of the eight pyrrole protons of the Mo(V)-appended model heme, $[TPPFe(2,3\text{-}MoOL)(N\text{-}MeIm)_2]^+$,[62] where L = hydrotris-(3,5-dimethylpyrazolyl)borate, counterrotation of the **g** tensor was not taken into account in that case; doing so reverses the sign and changes the relative magnitude of the rhombic dipolar (pseudocontact) shift at each position. The new values, for protons *a*−*h*, are +2.7, −4.4, −2.7, +4.4, +2.7, −4.4, −2.7, +4.4 ppm, respectively, and the resulting corrected contact shifts are −22.4, −29.4, −26.1, −19.5, −23.3, −29.8, −25.6, −18.8 ppm, respectively. These changes do not alter the basic conclusions reached in that work, and the corrected contact shifts *better* match the Hückel calculations reported therein for the eight protons (last column of Table 4 of that work[62]).

Magnetic Axis Orientations with Respect to the Heme in Ferriheme Proteins Determined by Single-Crystal EPR Spectroscopy. The orientations of the **g** tensor as determined by single-crystal EPR spectroscopy have been reported for only two heme proteins: cytochrome *c*[34] and metmyoglobin cyanide.[35,36] The results are included in Table 1, along with results obtained from NMR techniques, described below, and are mixed. The orientation of the **g** tensor of cytochrome *c*, reported by Mailer and Taylor,[34] agrees very well with both the predictions of the present work, which are based upon counterrotation of the in-plane **g** tensor and the known orientation of the histidine and methionine ligands determined by X-ray crystallography,[63] and with solution NMR results for the same protein (Table 1). Specifically, the −95° orientation of χ_{xx} is reasonably close to the average orientation of the nodal planes of the two axial ligands (−71°), and even closer to the orientation of the nodal plane of the methionine-filled π-symmetry p orbital (−93°). As mentioned further below, there has been some discussion in the literature as to whether the methionine dominates the orientation of the in-plane **g** tensor, or whether the histidine and methionine ligands contribute equally.

For sperm whale cyanometmyoglobin there have been two reports of the orientation of the **g** tensor,[35,36] and neither of them are consistent with either the predictions based upon counter-rotation of the in-plane **g** tensor presented herein, or with results obtained from NMR spectroscopy (Table 1). For myoglobin, the axial histidine plane is oriented about −10° to the *x*, or N_2-Fe-N_4 axis, Figure 1, suggesting that g_{xx} should be oriented at an angle of about +10° to that same axis. However, Hori reported the orientation of g_{xx} to be at −59° to the *x* axis,[35] while Peisach and co-workers reported g_{xx} to be at +78° to the same axis.[36] Results obtained by NMR spectroscopy, discussed below (−10° and −9°, Table 1), are closer to the prediction based upon counter-rotation, but still deviate by some 19−20° from that prediction.

Magnetic Axis Orientations with Respect to the Heme in Ferriheme Proteins Determined by Solution NMR Spectroscopic Techniques. For **g** tensor orientations determined by NMR spectroscopy, there has been some diversity in the orientations determined for the same protein in different laboratories. For NMR studies, the Euler angles α, β, and γ are usually used to define the relationship between the heme normal and in-plane *x* and *y* axes and the determined principal directions of the **g** tensor. In this definition β represents the deviation of the magnetic *z* axis from the normal to the heme plane and the sum $\alpha + \gamma = \kappa$ represents the approximate in-plane rotation of χ_{xx} and χ_{yy} from the *x* and *y* axes as defined by the authors, assuming β is small. (The magnetic susceptibilities χ_{xx} and χ_{yy} at the temperatures of the NMR investigations may or may not be directly proportional to the low-temperature EPR determined values of g_{xx}^2 and g_{yy}^2, depending on the importance of second-order Zeeman[64] and other contributions at the temperatures at which NMR measurements are made.) Unfortunately, not all research groups have used the same axis system, and in some cases, the axis system used is not clearly defined in the published paper.

In Table 1 we have collected the Euler angles for a number of well-studied heme proteins. For purposes of clarity we have redefined the axis system, where necessary, to a common reference frame in which the reference *x* axis of the molecule is defined as passing through the nitrogens of pyrrole rings II and IV of the heme and the *y* axis through the nitrogens of pyrrole rings I and III (Figure 1), a right-hand coordinate system. Because of this redefinition, the Euler angles α and γ, which are directly related to the particular axis system used, have not been tabulated. However, their sum, κ, can readily be redefined in our reference coordinate system, assuming that the deviation of the *z* magnetic axis from the heme normal, β, is small. For the same reason, only the absolute value of β has been tabulated in Table 1. As can be seen, the *z* magnetic axis is seldom exactly along the heme normal, although the deviations are usually not larger than 16° (but note HRPCN), and there is considerable variation in the orientation of the in-plane magnetic axes, κ_{obs}, with respect to the *x* and *y* axes defined in Figure 1. (In our terminology, κ_{obs} should equal γ, Figure 1.) The magnetic axis, χ_{xx} defines the direction of the *minimum* in-plane magnetic susceptibility direction; it is from this axis and the line connecting the metal to each individual proton of the heme (or, in fact, the entire protein) that the angle Ω, from which the cos 2Ω part of the dipolar (pseudocontact) shift[65] is calculated, is measured.

(58) Shokhirev, N. V.; Shokhireva, T. Kh.; Polam, J. R.; Watson, C. T.; Raffii, K.; Simonis, U.; Walker, F. A. *J. Phys. Chem. A* **1997**, *101*, 2778.
(59) Momot, K. I.; Walker, F. A. *J. Phys. Chem. A* **1997**, *101*, 2787.
(60) Polam, J. R.; Shokhireva, T. Kh.; Raffii, K.; Simonis, U.; Walker, F. A. *Inorg. Chim. Acta* **1997**, *263*, 109.
(61) Scheidt, W. R. Personal communication.
(62) Basu, P.; Shokhirev, N. V.; Enemark, J. H.; Walker, F. A. *J. Am. Chem. Soc.* **1995**, *117*, 9042.
(63) Berghuis, A. M.; Brayer, G. D. *J. Mol. Biol.* **1992**, *223*, 959.
(64) (a) Horrocks, W. D.; Greenberg, E. S. *Biochim. Biophys. Acta* **1973**, *322*, 38. (b) Horrocks, W. D.; Greenberg, E. S. *Mol. Phys.* **1974**, *27*, 993.
(65) Kurland, R. J.; McGarvey, B. R. *J. Magn. Reson.* **1970**, *2*, 286.

Table 1. Orientation of the **g** Tensors of Several Heme Proteins As Determined by NMR Spectroscopy, As Compared to the Orientation of the Nodal Plane(s) of the Filled p_π Orbital(s) of the Axial Ligand(s)[a]

protein (variety, form)	orientation of node of axial L p_π orbital	$\|\beta\|$	Euler angles deg κ_{obs}[b]	Euler angles deg κ_{pred}[c]	ref
cytochrome b_5					
(bovine, A)	−45(H39)	12	∼15	45(H39)	8
	−26(H63)			26(H63)	
	−45(H39)	7	23	45(H39)	9
	−26(H63)			26(H63)	
	−45(H39)		∼15	45(H39)	10,12
	−26(H63)			26(H63)	
	−45(H39)		27[d]	45(H39)	4
	−26(H63)			26(H63)	
(rat, A)	−45(H39)	8[e]	20[e]	45(H39)	11
	−26(H63)			26(H63)	
	−45(H39)		33[d]	45(H39)	4
	−26(H63)			26(H63)	
(rat, B)	−45(H39)	9[e]	61[e]	45(H39)	11
	−64(H63)			64(H63)	
	−45(H39)		60[d]	45(H39)	4
	−64(H63)			64(H63)	
metmyoglobin CN					
(sperm whale)	∼−10	14	−10	10	3
	∼−10		−9[d]	10	4
	∼−10	13[f]	−58[f]	10	35
	∼−10	13[f]	78[f]	10	36
(*G. japonicus*)	∼−10	6	2	10	5
(*Aplysia*)	−35	8	∼28	35	6
horseradish peroxidase CN	∼95[g]	21.2	85	85	1
	∼95[g]		92[d]	85	2
lignin peroxidase CN	∼120	0.5	74	60	7
	∼120		∼70[d]	60	2
Met → Ala yeast cytochrome *c* CN	+48(H)		+48	−48	16
cytochrome c					
(horse heart)	∼93(M)		∼−85	−93 (M)	17
	+48(H)			−48 (H)	
				−71 (av)[h]	
	∼93(M)	15	−79	−93 (M)	13
	+48(H)			−48 (H)	
				−71 (av)[h]	
	∼93(M)		−95[e]	−93 (M)	34
	+48(H)			−48 (H)	
				−71 (av)[h]	
(yeast iso-1)	∼93(M)	6	−20	−93 (M)	14
	+48(H)			−48 (H)	
				−71 (av)[h]	
(*R. caps.* c_2)	∼93(M)	12	107 or −73	−93 (M)	15
	+48(H)			−48 (H)	
				−71 (av)[h]	
cytochrome c_{551}					
(*P. aerug.*)	∼+3(M)		∼−15	−3 (M)	17
	+48(H)			−48 (H)	
				−25 (av)[h]	

[a] A common axis system is used, with *x* aligned along the nitrogens of pyrrole rings II and IV and *y* aligned along those of pyrrole rings I and III of the heme, using a right-hand coordinate system (Figure 1). Because of redefinition of axis systems in a number of cases, the Euler angles α and γ are not presented, and β is reported as the absolute value. H and M refer to histidine and methionine. [b] $\kappa = \alpha + \gamma$; defines approximate angle of rotation of the *x* and *y* magnetic axes in a right-hand coordinate system, assuming β is small. [c] Value of κ predicted by counterrotation of the **g** tensor by an equal number of degrees. [d] Measured from the heme orbital mixing parameter Θ, assuming counterrotation of the **g** tensor, rather than from dipolar shifts of protein protons. [e] χ_{xx} and χ_{yy} as defined in the paper have been reversed to provide agreement with other workers. [f] Determined by single crystal EPR. [g] Ligand plane orientation taken from the structure of cytochrome *c* peroxidase.[69] [h] Average of the nodal planes of the histidine and methionine ligands.

For cytochrome b_5, where there are two axial histidines oriented at 19° angles to each other, counterrotation of χ_{xx} should place this minimum magnetic susceptibility tensor component at +45° if His-39 dominates, or at +26° if His-63 dominates the orientation of the magnetic susceptibility tensor. The variations in κ_{obs} are relatively small (ranging from ∼15 to 33° for the A heme orientation form of bovine cytochrome b_5, Table 1). Unfortunately, while most researchers have determined the orientation of the **g** tensor and have related it to the heme, few have related it to the orientation of the axial ligands with respect to the heme. We have attempted to do this in Table 1, using the structures deposited in the Brookhaven Protein Data Bank. We have used the projection of the ligand plane(s) of the imidazole ring(s) of histidine(s), or the perpendicular to the average projection of the CH_2-S and CH_3-S vectors of methionine on the heme plane to define these angles in Table 1.

In the two right-hand columns of Table 1 that relate to κ, the approximate number of degrees through which the in-plane magnetic axes have been observed to rotate (κ_{obs}) is compared with the predicted rotation (κ_{pred}), based upon the concept of counterrotation of the **g** tensor with equal but opposite rotation.

It can be seen that for cytochrome b_5 the agreement is best if His-63 is more important in determining the magnetic axes, as suggested by Banci, Pierattelli and Turner,[4] while the La Mar group has suggested that His-39 is more important[10,12] and the Guiles group has concluded that they are equally important.[11] If His-63 is more important, $\kappa_{pred} \sim 26°$, while various laboratories have measured values, κ_{obs}, of 15−27° for the bovine protein, form A.[4,8−10,12] If His-39 were more important, κ_{pred} should be 45°, and if the two are equally important, κ_{pred} is 36°, both of which are farther from the κ_{obs} values determined by various research groups. The magnetic axes determined for both of the heme isomers of the rat protein by the Guiles group[11] only agree with the predictions, based upon the structure of the bovine protein, if isomers A and B (or, equivalently, χ_{xx} and χ_{yy}) are reversed in definition, as has been done in Table 1. This reversal has been made in one,[66] but not the other[67] recent paper from that laboratory.

For sperm whale metmyoglobin cyanide, there is a wide range in the orientation of magnetic axes reported, the two single-crystal EPR results[35,36] of which do not agree with the predictions, based upon counterrotation of the **g** tensor, Table 1, as mentioned above, and the two NMR results ($\gamma_0 = -10°$, $\kappa_{obs} = -10°$ [3] or −9°,[4] $\kappa_{pred} = \gamma = +10°$) appear more consistent with corotation than with counterrotation of χ_{xx}, and the ligand field parameters calculated from the g values[35,36] *could* place this protein in the small corotation region of Figure 4. However, from the g values measured by EPR spectroscopy,[35] Δ_{31} is calculated to be only 3.71λ, or ≤ 1485 cm^{-1}, depending on the value of λ. To be in the corotation region bounded by the curved line 1 and straight line 2 of Figure 4, Δ_{53} and Δ_{43} would need to be less than double this value, which leads to much too small a predicted value for the total splitting of the d orbitals, Δ_{51}, of ≤ 4456 cm^{-1}. Such a small splitting of the d orbitals should certainly produce a high-spin complex, which is not observed. It is possible that the deviation of the NMR results from the predictions of counterrotation of the magnetic susceptibility tensor is a consequence of contributions from the off-axis binding of the cyanide ligand: The z magnetic axis is inclined at an angle of approximately 14° toward the *δ-meso* position[3] in this protein (Figure 1), which has the effect of lifting the direction of χ_{xx} out of the heme plane, toward the cyanide ligand, by an equal number of degrees. However, cytochrome b_5, which suffers an off-axis orientation of χ_{zz} of up to 12° (Table 1), does not appear to be affected in the same way as is metMbCN, and the values of κ_{pred} match those of κ_{obs}, without need for corrections due to the z axis tilt. The reasons for the 19−20° lack of agreement between the NMR results for κ_{pred} and κ_{obs} of metMbCN (Table 1) are thus not clear at this time and should be the subject of further study.

Among other His-CN$^-$-ligated proteins, *Aplysia* MbCN, which has a different orientation of the proximal histidine plane than do other myoglobins (Table 1),[6,68] agrees quite well with counterrotation predictions ($\kappa_{obs} = 28°$, $\kappa_{pred} = 35°$). For horseradish peroxidase cyanide, both reports show good agreement between the values of κ_{obs} and κ_{pred}, assuming that the orientation of the histidine plane is similar to that for cytochrome *c* peroxidase.[69] For lignin peroxidase cyanide, for which the angle of the proximal histidine is known from X-ray crystallography, the agreement between predicted and observed values of κ is also quite good (Table 1). For the cyanide complex of the Met → Ala mutant of yeast cytochrome *c*, which also has His-CN$^-$ ligation, the directions of g_{xx} and g_{yy} are reversed from those expected based upon the orientation of the axial histidine[16] and counterrotation of the **g** tensor. The authors pointed out this discrepancy in their paper. This is another case where the g values reported ($g_{zz} \approx 3.30$, $g_{yy} \approx 2.0$, $g_{xx} \approx 1.07$ (calculated, assuming $\sum g^2 = 16$))[70] lead to calculated values of Δ_{31} that are very small (3.79λ, or ≤ 1520 cm^{-1}). If this were a case of corotation of the **g** tensor, Δ_{53} and Δ_{43} would both have to be less than $2\Delta_{31}$, leading to the conclusion that Δ_{51} must be ≤ 4560 cm^{-1}. Again, as in the case of metMbCN, this seems much too small for a low-spin complex. Hence, corotation is probably not occurring here, and some reinterpretation of the data may be in order.

For various cytochromes *c* the agreement is fair for horse heart *c*[13,17] and *P. aeruginosa* c_{551},[17] although it is difficult to conclude whether the histidine and methionine ligands contribute fairly equally to the orientation of the magnetic axes, as suggested previously.[17] In the case of Turner's work,[17] however, the values of κ_{obs} reported are those *based upon the assumption of counterrotation*, so the agreement is not surprising. However, it is clear that the agreement is not good for yeast iso-1 cytochrome *c*.[14] For *R. capsulatus* cytochrome c_2,[14] the direction of χ_{xx} is either consistent (−73°) or inconsistent (107°) with the predictions based upon counterrotation, depending on which way the χ_{xx} vector is pointing.

Although there is some scatter in the data reported in Table 1, it appears that at least in the majority of cases, the orientation of the magnetic axes observed by NMR spectroscopy is fairly similar to that predicted by equal and opposite rotation of the **g** or χ tensor with rotation of the axial ligands, and that for cyochrome b_5, His-63 appears to be most important in determining the orientation of the **g** tensor. For cytochrome *c*, it is not yet clear if the histidine and methionine ligands are equally important in determining this orientation, as previously suggested by Turner.[17]

In terms of the temperature dependence of the proton resonances of model hemes or heme proteins that have a thermally accessible excited state,[71] typically one that is oriented at right angles to the ground-state orbital, counterrotation of the **g** tensor does not change the expected (non-Curie) temperature dependence, although the calculation of molecular orbital coefficients obtained for the ground- and excited-state orbitals would have to be corrected by proper calculation of the dipolar (pseudocontact) contributions to the ground and excited states, considering the existence of counterrotation.

Despite the variations in findings of the orientation of the **g** tensor of heme proteins with respect to axial ligand orientation, we feel that if the finding of counterrotation of the in-plane **g** tensor for the systems discussed above is a general rule for heme proteins, as it appears to be, this information should be quite helpful in checking the reasonableness of magnetic axes determined for new heme proteins. Further study of cyanide-ligated heme proteins is in order, to determine whether corotation may occur in some of these systems, such as metMbCN and M80A cytochrome *c* CN. Because of the large number of degrees of freedom that exist in the determination of magnetic axes by NMR spectroscopy, such a check should be an aid in preventing erroneous orientations from being reported. It is to be hoped that in future reports of the determination of the

(66) Sarma, S.; DiGate, R. J.; Goodin, D. B.; Miller, C. J.; Guiles, R. D. *Biochemistry* **1997**, *36*, 5658.

(67) Sarma, S.; Dangi, B.; Yan, C. H.; DiGate, R. J.; Barville, D. L.; Guiles, R. D. *Biochemistry* **1997**, *36*, 5645.

(68) Bolognesi, M.; Onesti, S.; Gatti, G.; Coda, A.; Ascenzi, P.; Brunori, M. *J. Mol. Biol.* **1989**, *205*, 529.

(69) Edwards, S. L.; Poulos, T. L. *J. Biol. Chem.* **1990**, *265*, 2588.

(70) Bren, K. L.; Gray, H. B.; Banci, L.; Bertini, I.; Turano, P. *J. Am. Chem. Soc.* **1995**, *117*, 8067.

(71) Shokhirev, N. V.; Walker, F. A. *J. Phys. Chem.* **1995**, *99*, 17795.

magnetic axes of heme proteins by NMR spectroscopy, care will be taken to clearly define the orientation of the chosen reference frame and the determined magnetic axes directions within that reference frame, and that the directions determined will be checked with respect to the concept of counter-rotation of the **g** or χ tensor, so that true violations of this concept, if they exist, can be detected and studied to find the reasons for the violations.

Acknowledgment. The support of National Institutes of Health grant DK 31038 (F.A.W.) is gratefully acknowledged. F.A.W. thanks Dr. Roberta Pierattelli for helpful comments on this manuscript and for assistance in measuring the orientations of the axial ligands from structures deposited in the Brookhaven Protein Data Bank presented in Table 1.

JA972265S